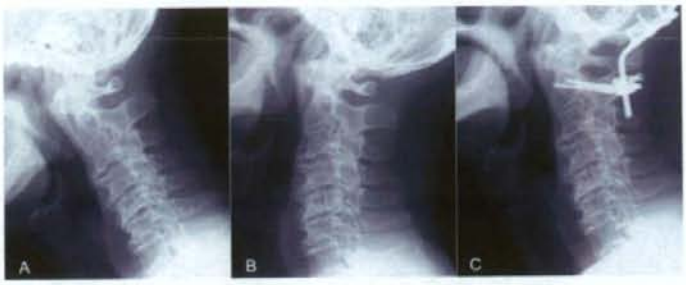

Figure 1. Preoperative radiographs of a 73-year-old man (patient 8) revealed extensive OALL. Atlantoaxial instability was not evident in flexion (**A**) and extension (**B**). The patient underwent O-C2 fusion with C1 laminectomy (**C**).

ROM was noted (mean, 17.6°; range, 3°-36°), especially in the patients with OALL. Further analysis of the segmental motion revealed ankylosis in O-C1 in 4 patients (including 1 patient with atlanto-occipital assimilation) and C2–C3 in 6 patients. Furthermore, CT revealed severe degenerative changes of the C2 to C3 zygapophysial joint in 4 patients (Figure 2).

All but 1 patient were treated with posterior occipitocervical fusion using pedicle screws (Table 3). Surgical procedures included O-C2 fusion (6 patients), O-C4 fusion(3 patients), and direct tumor resection by the lateral approach(1 patient). Additional C1 laminectomy was performed in all patients who underwent posterior fusion except 1 patient in whom adequate decompression was confirmed with intraoperative ultrasonography. There was no documented complication during perioperative period except that 1 patient had acute coronary syndrome, which required subsequent intervention. Neurologic status improved after surgery in all but 1 patient who was suffering from esophageal cancer. Preoperative upper m-JOA score (median, 2; range, 1–3) improved after surgery (median, 3.5; range, 1–4). Similarly, lower m-JOA score (median, 2; range, 1–3) also improved after surgery (median, 3; range, 2–4). Follow-up MRI was available in 8 patients. In the remaining 2 patients, deteriorated health status due to unrelated diseases (esophageal cancer and pneumonia, respectively) precluded further study. MRI revealed the regression of the pseudotumors in all patients and decompression of the spinal cord (Figure 3). Regression of the pseudotumors was confirmed by emergence of the subarachnoid space in postoperative MRI and further evidenced by reduction in thickness of the retro-odontoid soft tissue (3.4 ± 0.8 mm; range, 2.3-4.7 mm).

■ Discussion

Our study had 3 main findings. First, we have shown that the retro-odontoid pseudotumors can develop without overt atlantoaxial instability. Second, we found marked decrease in subaxial ROM, mainly because of extensive OALL. Furthermore, most of the patients had ankylosis of O-C1 or C2 to C3, the segments adjacent to the atlantoaxial joint. Finally, spontaneous mass regression occurred after posterior fusion even in the absence of radiographic atlantoaxial instability.

The retro-odontoid pseudotumor has been generally considered as a rare sequela of atlantoaxial subluxation. In the postulated view on its pathomechanism, preexisting atlantoaxial instability was presumed to cause repeated tear and subsequent hypertrophy of the transverse ligament,[4,16] thus leading to the formation of the pseudotumor. The current study, however, revealed that the retro-odontoid pseudotumors were not necessarily associated with overt atlantoaxial instability. This finding indicates a different view on the formation of the pseudotumor: In the first place, excessive stress concentration to the atlantoaxial complex, due to altered biomechanics of the cervical spine, may repeatedly cause damage to the transverse ligament. A reactive mass may develop gradually after cycles of repetitive injuries to the ligament and reparative process. Although atlantoaxial subluxation might ensue from further attenuation of the

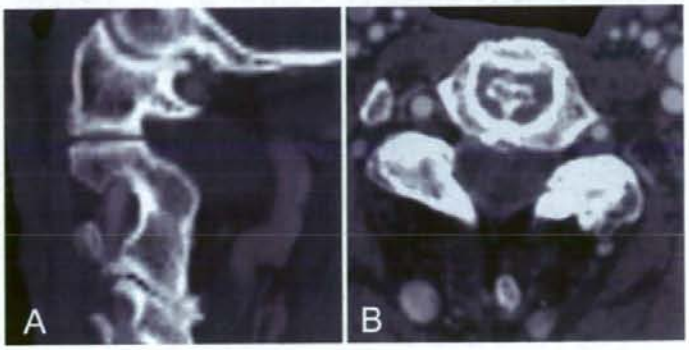

Figure 2. Sagittal (**A**) and axial (**B**) CT reconstructions (both from patient 8) demonstrated severe spondylosis in bilateral C2 to C3 zygapophysial joints.

Table 3. Outcome of Surgical Treatment

Patient No.	Surgery	Preoperative m-JOA		Postoperative m-JOA		Outcome	Follow-up MRI
		Upper	Lower	Upper	Lower		
1	Partial removal, O-C2 fusion, C1 laminectomy	1	1	2	2	Improved	Regression
2	Direct removal	2	1	4	4	Improved	Extirpated
3	O-C4 fusion, C1 laminectomy	1	2	3	3	Improved	N.A.*
4	O-C2 fusion, C1 laminectomy	1	2	3	3	Improved	Regression
5	O-C4 fusion, C1 laminectomy	1	2	1	2	Unchanged	N.A.*
6	O-C2 fusion, C1 laminectomy, C3–C7 laminoplasty	2	2	3	2	Improved	Regression
7	O-C2 fusion, C3–C7 laminoplasty	3	2	4	4	Improved	Regression
8	O-C2 fusion, C1 laminectomy	3	3	4	4	Improved	Regression
9	O-C2 fusion, C1 laminectomy	2	2	4	4	Improved	Regression
10	O-C4 fusion, C1–C2 laminectomy	2	2	4	3	Improved	Regression

*Deterioration of the patient's condition due to unrelated diseases precluded the follow-up MRI study.
Upper, indicates upper extremities; Lower, lower extremities; N.A., not available.

ligamentous structure, atlantoaxial instability should be viewed as a consequence of the degeneration process, not a prerequisite for the formation of the pseudotumor.

We found that extensive OALL was highly prevalent in patients with retro-odontoid pseudotumors. Modified stress distribution secondary to extensive OALL has been implicated in the literature as possible pathomechanism. Jun *et al* reported a case with diffuse idiopathic skeletal hyperostosis and attributed its cause to loss of mobility of subaxial segments and the secondary transfer of mechanical stress to the atlantoaxial segment.[16] Patel *et al* reported 5 patients of a retro-odontoid mass associated with Forestier disease, speculating that multilevel subaxial fusion because of OALL coupled with the mobility of the craniovertebral joint complex plays a pivotal role in the development of the mass.[15] In line with these reports, the current study demonstrated extensive OALL and marked decrease in subaxial ROM in patients with a retro-odontoid pseudotumor. Our data indicate that altered biomechanics of the cervical spine because of OALL plays a role in formation of the retro-odontoid pseudotumor.

Ankylosis of the segments adjacent to the atlantoaxial joint was another characteristic finding associated with retro-odontoid pseudotumors. Loss of mobility at the adjacent segment is known to contribute to increased risk of atlantoaxial dysfunction in other chronic condi-

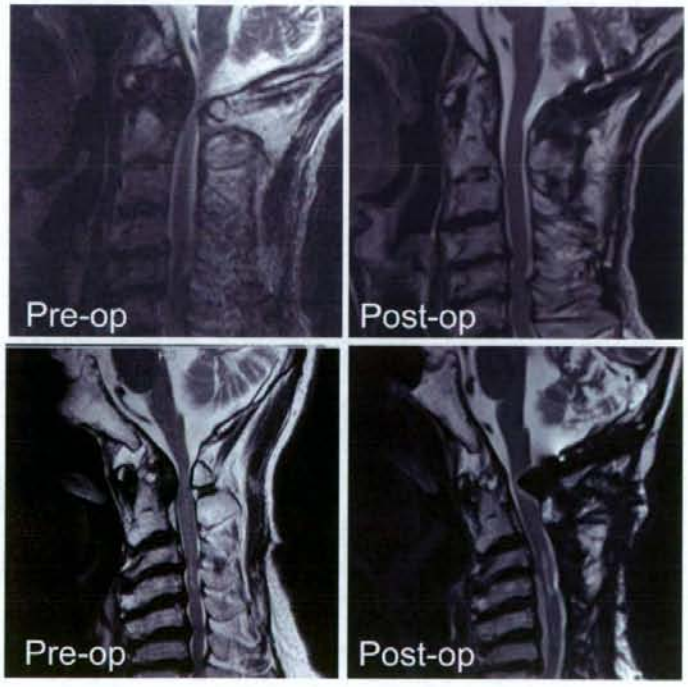

Figure 3. Preoperative and postoperative T2-weighted MR images of patient 8 (upper panels) and patient 6 (lower panels). Spontaneous regression of the mass lesion occurred after posterior fusion.

tions. In patients with Klippel-Feil syndrome, in which the C2 to C3 is the most commonly fused level, subsequent stress transfer at the C1 to C2 segment has been suggested as a risk factor for atlantoaxial instability. Shen *et al* have shown that occipitalization combined with a fused C2 to C3 segment results in the greatest amount of atlantoaxial instability in patients with Klippel-Feil syndrome.[18] Our results suggest that the altered dynamics of the cervical spine, especially those in the adjacent segments —O-C1 and C2 to C3—play a crucial role in the development of the retro-odontoid pseudotumor, indicating that the mass develops as an adjacent segment disease.

Optimal treatment for a retro-odontoid pseudotumor that is not associated with atlantoaxial instability has not been established, although transoral removal has usually been employed in such a case. In this study, 3 types of surgical procedures were used: extirpation of the mass, O-C2 fusion, and O-C4 fusion. We performed extirpation only in the earlier period when posterior fusion was not known to be effective. Afterward, we used posterior fusion as the treatment of choice. We preferred occipito-cervical fusion to C1 to C2 fusion because of ample space for bone grafting even after the resection of C1 posterior arch, which was performed in most cases. We usually extended fusion down to C4 when safety of inserting C2 pedicle screws was in doubt because of the anatomic limitations such as high riding vertebral artery, identified by preoperative planning using CT navigation system. In the current study, we have shown that posterior fusion invariably produced mass regression even in cases without radiographic atlantoaxial instability. This previously undocumented finding may be attributable to the fact that posterior fusion greatly reduces stress concentration to the atlantoaxial junction. Considering that the reactive mass develops as an adjacent segment disease, relieving mechanical stress at the atlantoaxial junction is a reasonable strategy for preventing further progression of the disease. Our data indicate that posterior fusion is the treatment of choice even for cases without overt atlantoaxial instability.

There are several limitations to the present study. Although this is the largest case series, we need to examine more cases to determine the precise incidence of the radiographic characteristics we mentioned. Moreover, a cohort or case-control study is required to further demonstrate the cause-effect relationship of the putative risk factors we discussed in the present study. Retro-odontoid pseudotumors occur only in a fraction of population with OALL or having ankylosis of O-C1 or C2 to C3, which may be partly attributable to variable biologic responses of the ligamentous tissue among the individuals. Further studies are needed to clarify the role of other biologic or genetic factors that predispose patients to development of retro-odontoid pseudotumors.

■ Conclusion

Retro-odontoid pseudotumors were not always associated with radiographic atlantoaxial instability. Our results suggest that extensive OALL and ankylosis of the adjacent segments are risk factors for the formation of pseudotumors. The retro-odontoid pseudotumors may develop as an adjacent segment disease after altered biomechanics of the cervical spine, especially those in the adjacent segments. Posterior fusion is the treatment of choice even for cases without radiographic atlantoaxial instability.

■ Key Points

- Retro-odontoid pseudotumors were not necessarily associated with radiographic atlantoaxial instability.
- Subaxial fusion due to OALL and ankylosis of the adjacent segments (O-C1, C2–C3) may be risk factors for the formation of the pseudotumor.
- Posterior fusion resulted in spontaneous regression of the pseudotumor even in cases without radiographic atlantoaxial instability.

References

1. Oohori Y, Seichi A, Kawaguchi H, et al. Retroodontoid pseudotumor resected by a high cervical lateral approach in a rheumatoid arthritis patient: a case report. *J Orthop Sci* 2004;9:90–3.
2. Crockard HA, Sett P, Geddes JF, et al. Damaged ligaments at the craniocervical junction presenting as an extradural tumour: a differential diagnosis in the elderly. *J Neurol Neurosurg Psychiatr* 1991;54:817–21.
3. Sze G, Brant-Zawadzki MN, Wilson CR, et al. Pseudotumor of the craniovertebral junction associated with chronic subluxation: MR imaging studies. *Radiology* 1986;161:391–4.
4. Yoshida MT, Kawakami M, Natsumi K, et al. Retro-odontoid pseudotumor associated with chronic atlanto-axial instability. *Rinsho Seikei Geka* 1995; 30:395–402 [in Japanese].
5. Yamashita K, Aoki Y, Hiroshima K. Myelopathy due to hypoplasia of the atlas: a case report. *Clin Orthop Relat Res* 1997;90–3.
6. Yamaguchi I, Shibuya S, Arima N, et al. Remarkable reduction or disappearance of retroodontoid pseudotumors after occipitocervical fusion: report of three cases. *J Neurosurg Spine* 2006;5:156–60.
7. Jun BY. Complete reduction of retro-odontoid soft tissue mass in os odontoideum following the posterior C1–C2 tranarticular screw fixation. *Spine* 1999;24:1961–4.
8. Lagares A, Arrese I, Pascual B, et al. Pannus resolution after occipitocervical fusion in a non-rheumatoid atlanto-axial instability. *Eur Spine J* 2006;15: 366–9.
9. Lansen TA, Kasoff SS, Tenner MS. Occipitocervical fusion for reduction of traumatic periodontoid hypertrophic cicatrix: case report. *J Neurosurg* 1990;73:466–70.
10. Rabadan AT, Sevlever G. Hypertrophic atlantoaxial ligaments: an unusual cause of compression of the upper spinal cord. *J Neurol Neurosurg Psychiatr* 2000;68:116–17.
11. Komatsu Y, Shibata T, Yasuda S, et al. Atlas hypoplasia as a cause of high cervical myelopathy: case report. *J Neurosurg* 1993;79:917–19.
12. Chen TY, Lui TN. Retrodental fibrocartilaginous mass: report of a case. *Spine* 1997;22:920–3.
13. Sato K, Kubota T, Takeuchi H, et al. Atlas hypoplasia associated with nontraumatic retro-odontoid mass. *Neurol Med Chir (Tokyo)* 2006;46:202–5.
14. Suetsuna F, Narita H, Ono A, et al. Regression of retroodontoid pseudotumors following C-1 laminoplasty: report of three cases. *J Neurosurg Spine* 2006;5:455–60.
15. Patel NP, Wright NM, Choi WW, et al. Forestier disease associated with a retroodontoid mass causing cervicomedullary compression. *J Neurosurg* 2002;96:190–6.
16. Jun BY, Yoon KJ, Crockard A. Retro-odontoid pseudotumor in diffuse idiopathic skeletal hyperostosis. *Spine* 2002;27:E266–70.
17. White AA, Panjabi, MM. *Clinical Biomechanics of the Spine*. 2nd ed. Philadelphia: Lippincott Williams and Wilkins; 1990.
18. Shen FH, Samartzis D, Herman J, et al. Radiographic assessment of segmental motion at the atlantoaxial junction in the Klippel-Feil patient. *Spine* 2006;31:171–7.

Effects of mobility/immobility of surface modification by 2-methacryloyloxyethyl phosphorylcholine polymer on the durability of polyethylene for artificial joints

Masayuki Kyomoto,[1,2] Toru Moro,[3] Fumiaki Miyaji,[1] Masami Hashimoto,[4] Hiroshi Kawaguchi,[3] Yoshio Takatori,[3] Kozo Nakamura,[3] Kazuhiko Ishihara[2,5]

[1]*Research Department, Japan Medical Materials Corporation, Osaka, Japan*
[2]*Department of Materials Engineering, School of Engineering, The University of Tokyo, Tokyo, Japan*
[3]*Department of Orthopaedic Surgery, School of Medicine, The University of Tokyo, Tokyo, Japan*
[4]*Materials Research and Development Laboratory, Japan Fine Ceramics Center, Nagoya, Japan*
AQ1 [5]*Center for NanoBio Integration, The University of Tokyo, Tokyo, Japan*

Received 11 December 2007; revised 29 February 2008; accepted 27 March 2008
Published online 00 Month 2008 in Wiley InterScience (www.interscience.wiley.com). DOI: 10.1002/jbm.a.32092

Abstract: Surface modification is important for the improvement in medical device materials. 2-Methacryloyloxyethyl phosphorylcholine (MPC) polymers have attracted considerable attention as surface modifiable polymers for several medical devices. In this study, we hypothesize that the structure of the surface modification layers might affect the long-term stability, hydration kinetics, wear resistance, and so forth, of medical devices such as artificial joints, and the poly(MPC) (PMPC) grafted surface might assure the long-term performance of such devices. Therefore, we investigate the surface properties of various surface modifications by using dip coatings of MPC-*co*-*n*-butyl methacrylate (PMB30) and MPC-*co*-3-methacryloxypropyl trimethoxysilane (PMSi90) polymers, or photoinduced radical grafting of PMPC and also the effects of the surface properties on the durability of cross-linked polyethylene (CLPE) for artificial joints. The PMPC-grafted CLPE has an extremely low and stable coefficient of dynamic friction and volumetric wear as compared to the untreated CLPE, PMB30-coated CLPE, and PMSi90-coated CLPE. It is concluded that the photoinduced radical graft polymerization of MPC is the best method to retain the benefits of the MPC polymer used in artificial joints under variable and multidirectional loads for long periods with strong bonding between the MPC polymer and the CLPE surface, and also to retain the high mobility of the MPC polymer. © 2008 Wiley Periodicals, Inc. J Biomed Mater Res 00A: 000–000, 2008

Key words: joint replacement; polyethylene; phosphorylcholine; surface modification; wear mechanism

INTRODUCTION

Polymeric biomaterials are widely used in the biomedical field for manufacturing artificial organs, medical devices, and disposable clinical apparatus.[1,2] Advancements in the biomedical field also demand substantial improvements in polymeric biomaterials. Conventional single-component polymer biomaterials cannot satisfy these requirements. Multicomponent polymer systems have therefore been designed and prepared for new multifunctional biomaterials.

Surface modification is one of the important means of preparing new multifunctional biomaterials. 2-Methacryloyloxyethyl phosphorylcholine (MPC) polymers have attracted considerable attention as surface-modifiable polymers for several medical devices.[3–11] MPC, a methacrylate with a phospholipid polar group in the side chain, is a monomer for preparing novel polymer biomaterials. An excellent synthetic route for MPC has been developed by Ishihara et al.[12] MPC can undergo conventional radical copolymerization with other methacrylate and styrene derivatives such as *n*-butyl methacrylate (BMA), *n*-dodecyl methacrylate (DMA), and 3-methacryloxypropyl trimethoxysilane (MPSi) to form poly(MPC-*co*-BMA), poly(MPC-*co*-DMA), and poly (MPC-*co*-MPSi), respectively.[5–11] These MPC polymers are some of the most common biocompatible

Correspondence to: M. Kyomoto, Uemura Nissei Bldg. 9F, 3-3-31 Miyahara, Yodogawa-ku, Osaka 532-0003, Japan; e-mail: kyomotom@jmmc.jp

Contract grant sponsor: Japanese Ministry of Education, Culture, Sports, Science and Technology; contract grant number: 15390449
Contract grant sponsor: Japanese Ministry of Health, Labor and Welfare
AQ3

J_ID: ZA1 Customer A_ID: 07-1024.R1 Cadmus Art: JBMA32092 Date: 23-APRIL-08 Stage: I Page: 2

and hydrophilic polymers studied thus far. They have potential applications in a variety of fields such as biology, biomedical science, and surface chemistry, because they possess unique properties such as good biocompatibility, high lubricity and low friction, antiprotein adsorption, and cell membrane-like surfaces. Several medical devices have already been developed by utilizing the MPC polymers and used clinically; therefore, the efficacy and safety of the MPC polymers as biomaterials are well established.[2–11]

When a natural joint in the human body ceases to function, for example, due to disease, trauma, or overuse, an artificial joint replacement often becomes necessary. There is a substantial increase in the number of artificial hip and knee joints used worldwide each year for primary and revised hip and knee joint replacements.[13] This indicates that a higher quality and longer lifetime have been increasingly desired for artificial joint replacements. Normally, artificial joints allow the body to regain mechanical and biological functions. Medical implants must be adapted to the dynamic loads experienced during use, and they must have the desired long-term biological interaction with the surrounding tissue. A typical artificial joint replacement system used as a medical device comprises a metallic surface made of a cobalt-chromium-molybdenum (Co-Cr-Mo) alloy that articulates against an ultra-high molecular weight polyethylene (UHMWPE) polymeric component. However, the artificial joint replacements are subjected to adhesive and abrasive wear, and both metallic and polymeric debris. These are known to produce a variety of cytokines and tumor necrosis factors that progressively resorb the bone by osteolysis, leading to aseptic loosening of the artificial joint after a number of years, which is recognized as a serious problem.[14,15] Different combinations of bearing surfaces and improvements in bearing materials have been studied with the aim of reducing the number of UHMWPE wear debris that induce osteolysis.[16–18]

Recently, we have developed an artificial hip joint by using poly(MPC) (PMPC) grafted onto the surface of cross-linked polyethylene (CLPE; PMPC-grafted CLPE); this device is designed to reduce wear and suppress bone resorption.[19–24] MPC has also been directly grafted from biomaterial surfaces through photoinduced radical polymerization.[25,26] This photoinduced radical polymerization facilitates the direct grafting of MPC onto biomaterial surfaces. The following are the expected advantages of this technique: (1) controllable graft polymer density and length and grafting site,[21,24] (2) covalent bonding between the graft polymer and biomaterial surfaces (as high immobility), which assures the long-term stability of graft chains, (3) high mobility of the graft polymer chain and/or free end groups of the polymer, and (4) occurrence of grafting only on the surface, and no effect of grafting on the bulk properties.[22] In particular, strong bonding between the surface modification and the surface is an important issue, which is associated with the long-term retention of the benefits of the surface modification used in artificial joints under variable and multidirectional loads, for a promising long-term performance of artificial joints.

In this study, we hypothesize that the structure of surface modification layers might affect the surface density of the phosphorylcholine group, long-term stability and mobility of the polymer chain, hydration kinetics, and so forth, and the PMPC-grafted surface might assure the long-term performance of artificial joints. Therefore, we investigate the surface properties of various surface modification layers with the MPC polymer and the effects of the surface properties on the durability of the CLPE for artificial joints. The results reveal that the structure of the PMPC-grafted layer on the CLPE surface plays an important role in reducing the wear of the orthopedic bearing surface in the long term.

MATERIALS AND METHODS

Materials

MPC was industrially synthesized using a previously reported method.[12] Poly(MPC-*co*-BMA) (PMB30; MPC:BMA unit mole fraction = 0.3:0.7)[12] and poly(MPC-*co*-MPSi) (PMSi90; MPC:MPSi unit mole fraction = 0.9:0.1)[8] were synthesized in ethanol using 2,2'-azobisisobutyronitrile as initiator by a conventional radical copolymerization method. A compression-molded UHMWPE (GUR1020 resin; Poly Hi Solidur, IN) sheet stock was irradiated with 50 kGy γ-rays in N_2 gas and annealed at 120 C for 7.5 h in N_2 gas in order to achieve cross-linking. The CLPE specimens were machined from this sheet stock after cooling.

MPC polymer coating

The preparation of the MPC polymer coated CLPE is schematically illustrated in Figure 1. The physical coating of PMB30 was carried out by the solvent evaporation method, where the CLPE specimens were dipped into ethanol solution containing 0.2 mass % PMB30 for 10 s for coating, and then placed in an ethanol vapor atmosphere at room temperature for 1 h. The coated CLPE specimens were again dipped for 10 s and placed in the ethanol vapor atmosphere at room temperature for 1 h (PMB30-coated CLPE). F1

The chemical coating of PMSi90 was also carried out by the solvent evaporation method. Before the PMSi90 coating, the CLPE specimens were irradiated with O_2 plasma at a 200 W high-frequency output and 150 mL/min O_2 gas flow for 2 min by using an O_2 plasma etcher (PR500,

ID: vasanss Date: 23/4/08 Time: 21:11 Path: J:/Production/JBMM/Vol00000/080210/3B2/C2JBMM080210

J_ID: ZA1 Customer A_ID: 07-1024.R1 Cadmus Art: JBMA32092 Date: 23-APRIL-08 Stage: I Page: 3

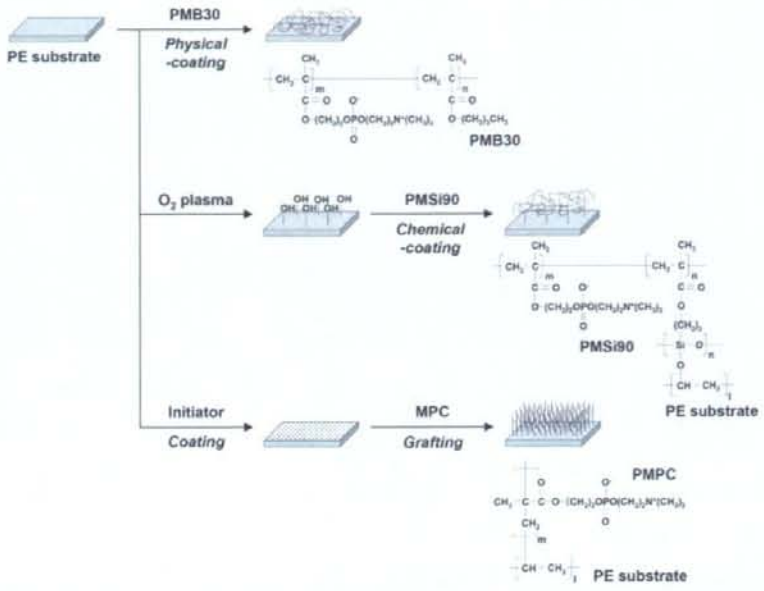

Figure 1. Scheme for the preparation of MPC polymer-coated CLPE and PMPC-grafted CLPE.

Yamato Scientific Co., Tokyo, Japan). The O_2 plasma irradiation formed the surface hydroxide layer. The CLPE specimens were dipped into ethanol solution containing 0.5 mass % PMSi90 and 0.063 mg/mL succinic acid (Kanto Chemical Co., Tokyo, Japan) for 10 s for the silanization of trimethoxysilane group of PMSi90 and placed in the ethanol vapor atmosphere at room temperature for 1 h. The coated CLPE specimens were annealed in air at 70 C for 3 h for dehydration (PMSi90-coated CLPE). These PMB30- and PMSi90-coated CLPE specimens were then sterilized by 25 kGy γ-rays in N_2 gas.

MPC graft polymerization

The preparation of the PMPC-grafted CLPE is schematically illustrated in Figure 1. The CLPE specimens were immersed in acetone (Wako Pure Chemical Industries, Osaka, Japan) solution containing 10 mg/mL benzophenone (Wako Pure Chemical Industries) for 30 s, and then dried in the dark at room temperature in order to remove the acetone. In previous studies, using ultraviolet spectroscopy, the amount of benzophenone adsorbed on the surface was reported to be 3.5×10^{-11} mol/cm^2.[3] MPC was dissolved in degassed pure water to obtain a concentration of 0.5 mol/L. Subsequently, the benzophenone-coated CLPE specimens were immersed in the aqueous MPC solutions. Photoinduced graft polymerization was carried out on the CLPE surface using ultraviolet irradiation (UVL-400HA ultra-high pressure mercury lamp; Riko-Kagaku Sangyo Co., Funabashi, Japan) with an intensity of 5 mW/cm^2 at 60 C for 90 min; a filter (model D-35; Toshiba Corp., Tokyo, Japan) was used to restrict the passage of ultraviolet light to wavelengths of 350 ± 50 nm. After the polymerization, the PMPC-grafted CLPE specimens were removed, washed with pure water and ethanol, and dried at room temperature. These specimens were then sterilized by 25 kGy γ-rays in N_2 gas.

Surface analysis

The functional group vibrations of the untreated CLPE, PMB30-coated CLPE, PMSi90-coated CLPE, and PMPC-grafted CLPE surfaces were examined using attenuated total reflection (ATR) by Fourier transform infrared (FTIR) spectroscopy. The FTIR/ATR spectra were obtained in 32 scans over a range of 800–2000 cm^{-1} by using an FTIR analyzer (FT/IR615; Jasco International Co., Tokyo, Japan) at a resolution of 4.0 cm^{-1}.

The surface elemental contents of the untreated CLPE, PMB30-coated CLPE, PMSi90-coated CLPE, and PMPC-grafted CLPE were analyzed using X-ray photoelectron spectroscopy (XPS). The XPS spectra were obtained using an XPS spectrophotometer (AXIS Hsi 165; Kratos Analytical Ltd., Manchester, UK) equipped with an Mg-Kα radiation source by applying a voltage of 15 kV at the anode. The take-off angle of the photoelectrons was maintained at 90°. Each measurement was scanned five times; five replicate measurements were performed for each sample, and the average values were considered for the surface elemental contents.

The static water-contact angles of the untreated CLPE, PMB30-coated CLPE, PMSi90-coated CLPE, and PMPC-grafted CLPE were measured using an optical bench-type contact angle goniometer (model DM300; Kyowa Interface

ID: vasanss Date: 23/4/08 Time: 21:11 Path: J:/Production/JBMM/Vol00000/080210/3B2/C2JBMM080210

J_ID: ZA1 Customer A_ID: 07-1024.R1 Cadmus Art: JBMA32092 Date: 23-APRIL-08 Stage: I Page: 4

Science Co., Saitama, Japan) by the sessile drop method. Drops of purified water (1 μL) were deposited onto the surface modified CLPE with MPC polymer, and the contact angles were directly measured after 60 s by using a microscope according to the ISO 15989 standard.[27] Subsequently, 15 replicate measurements were performed for each sample, and the average values were considered as the contact angles.

Cross-sectional observation by transmission electron microscopy

A cross-section of the PMB30, PMSi90, and PMPC layers on the CLPE surface was observed using a transmission electron microscope (TEM). The specimens were first embedded in epoxy resin, stained with ruthenium oxide vapor at room temperature, and then sliced into ultra-thin films (~100-nm thick) by using a Leica Ultra Cut UC microtome (Leica Microsystems, Wetzlar, Germany). A JEM-1010 electron microscope (JEOL, Tokyo, Japan) was used for the TEM observation at an acceleration voltage of 100 kV.

Characterization of protein adsorption by micro bicinchoninic acid method

The amount of protein adsorbed on the untreated CLPE, PMB30-coated CLPE, PMSi90-coated CLPE, and PMPC-grafted CLPE surfaces was measured by the micro bicinchoninic acid (BCA) method. Each specimen was immersed in Dulbecco's phosphate-buffered saline (PBS, pH 7.4, ion strength = 0.15*M*; Immuno-Biological Laboratories Co., Takasaki, Japan) for 1 h to equilibrate the surface modified by the MPC polymer. The specimens were immersed in bovine serum albumin (BSA, $M_w = 6.7 \times 10^4$; Sigma-Aldrich Corp., MO) solution at 37°C for 1 h. The protein solution was prepared in a BSA concentration of 4.5 g/L, that is, 10% of the concentration of the human plasma levels. Then, the specimens were rinsed five times with fresh PBS and immersed in 1 mass % sodium dodecyl sulfate (SDS) aqueous solution, and shaken at room temperature for 1 h to completely detach the adsorbed BSA on the surface modified by the MPC polymer. A protein analysis kit (micro BCA protein assay kit, No. 23235; Thermo Fisher Scientific, IL) based on the BCA method was used to determine the BSA concentration in the SDS solution, and the amount of BSA adsorbed on the surface modified by the MPC polymer was calculated.

Friction test

A friction test was performed using a ball-on-plate machine (Tribostation 32; Shinto Scientific Co., Tokyo, Japan). Each of the untreated CLPE, PMB30-coated CLPE, PMSi90-coated CLPE, and PMPC-grafted CLPE surfaces was used to prepare six sample pieces. A Co-Cr-Mo alloy ball with a diameter of 9 mm was prepared. The surface roughness of the ball was Ra $\geq$ 0.01, which was comparable to that of femoral ball products. The friction tests were performed at room temperature with various loads in the range of 0.49–9.80 N, sliding distance of 25 mm, and frequency of 1 Hz for a maximum of 100 cycles.[28] Pure water was used as a lubricant medium. The mean coefficients of dynamic friction were determined by averaging five data points from the 100 (96–100) cycle measurements.

Hip joint simulator wear test

A 12-station hip joint simulator (MTS Systems Corp., MN) with the untreated CLPE, PMB30-coated CLPE, PMSi90-coated CLPE, and PMPC-grafted CLPE cups (n = 2), both having inner and outer diameters of 26 and 52 mm, respectively, was used for the hip joint simulator wear test. A Co-Cr-Mo alloy femoral ball component with a size of 26 mm (Japan Medical Materials Corp., Osaka, Japan) was used as the femoral component. A mixture of 25 vol % bovine serum, 20 m*M*/L of ethylene diamine tetraacetic acid, and 0.1 mass % sodium azide was used as a lubricant, according to the ISO 14242-1 standard.[29] The lubricant was replaced every 0.5×10^6 cycles. Walks that simulated a physiologic loading curve (Paul-type), with double peaks at 1793 and 2744 N loads with a multidirectional (biaxial and orbital) motion of 1 Hz frequency, were applied. The wear was determined by weighing the cups at intervals of 0.5×10^6 cycles. Load-soak controls (n = 2) were used to compensate the fluid absorption by the specimens.[30] The testing was continued until a total of 3.0×10^6 cycles were completed.

Statistical analysis

The results derived from each measurement in the water-contact angle estimation, friction test, and protein adsorption test were expressed as mean values and standard deviation. The statistical significance ($p < 0.05$) was estimated by Student's t-test.

RESULTS

Figure 2 shows the FTIR/ATR spectra of the untreated CLPE, PMB30-coated CLPE, PMSi90-coated CLPE, and PMPC-grafted CLPE. An absorption peak was observed at 1460 cm^{-1} for all test specimens. This peak is mainly attributed to the methylene (CH_2) chain in the CLPE substrate and the MPC polymer chain. However, absorption peaks at 1240, 1080, and 970 cm^{-1} were observed only for the CLPE, whose surface was modified by the MPC polymer. These peaks corresponded to the phosphate group (P—O) in the MPC unit. Similarly, an absorption peak at 1720 cm^{-1} observed in the surface modified CLPE corresponded only to the carbonyl group (C=O) in the MPC unit. The absorption peak intensity of the P—O group of the PMPC-grafted CLPE was the highest in the CLPE, whose surface was modified by the MPC polymer. F2

ID: vasanss Date: 23/4/08 Time: 21:11 Path: J:/Production/JBMM/Vol00000/080210/3B2/C2JBMM080210

J_ID: ZA1 Customer A_ID: 07-1024.R1 Cadmus Art: JBMA32092 Date: 23-APRIL-08 Stage: I Page: 5

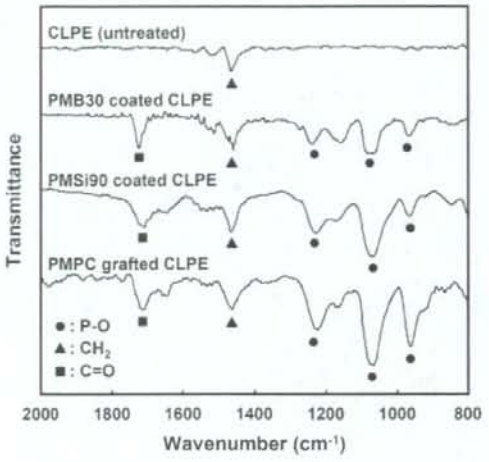

Figure 2. FTIR/ATR spectra of untreated CLPE, MPC polymer-coated CLPE, and PMPC-grafted CLPE.

T1 Table I summarizes the surface elemental compositions of the untreated CLPE, PMB30-coated CLPE, PMSi90-coated CLPE, and PMPC-grafted CLPE. The nitrogen (N) and phosphorous (P) contents in all the CLPE specimens, whose surface were modified by the MPC polymer, were observed. The surface elemental compositions of both N and P in the surface modified CLPE increased with an increase in the MPC composition in the polymer for surface modification. In particular, the elemental compositions of N and P in the PMPC-grafted CLPE surface were 5.2 and 5.3 atom %, respectively. The elemental composition of the PMPC-grafted CLPE surface was almost equivalent to the theoretical elemental composition ($N = 5.3$, $P = 5.3$ atom %) of PMPC.

F3 Figure 3 shows the cross-sectional TEM images of the untreated CLPE, PMB30-coated CLPE, PMSi90-coated CLPE, and PMPC-grafted CLPE. For the PMB30 and PMSi90 coatings, and PMPC grafting, a 100-nm thick MPC polymer layer was clearly observed on the surface of the CLPE substrate. No crack for poor adhesion and/or delamination was observed at the interface between MPC polymer layer and CLPE substrate. These results indicate that each surface modification layer on the CLPE substrate is uniform and cover closely, regardless of the binding conditions: the surface modification layers by the PMB30 and PMSi90 coatings, and PMPC grafting are combined with the substrate by physical adsorption and covalent bonds of Si—O—C and C—C, respectively. In the PMB30-coated CLPE, a bilayer structure attributed to dipping twice was clearly observed on the surface modification layer.

F4 Figure 4 shows the static water-contact angles of the untreated CLPE, PMB30-coated CLPE, PMSi90-coated CLPE, and PMPC-grafted CLPE. The static water-contact angles of the untreated CLPE and PMB30-coated CLPE were 90° and 100°, respectively, and they decreased markedly to ~10° (i.e., 8°–13°, $p < 0.001$) by the PMSi90 coating and PMPC grafting.

F5 Figure 5 shows the amount of BSA adsorbed on the surfaces of the untreated CLPE, PMB30-coated CLPE, PMSi90-coated CLPE, and PMPC-grafted CLPE. The amount of BSA adsorbed on the CLPE surface modified by the MPC polymer was considerably lesser ($p < 0.001$) than that of the untreated CLPE, that is, 0.05–0.10 μg/cm^2. These results imply that the surface modification by the MPC polymer results in good biocompatibility.

F6 Figure 6 shows the coefficients of dynamic friction of the untreated CLPE, PMB30-coated CLPE, PMSi90-coated CLPE, and PMPC-grafted CLPE. As compared to the untreated specimens, the PMB30-coated and PMSi90-coated CLPE specimens showed a reduction of ~30% (i.e., 25–30%, not significant) in their coefficients of dynamic friction. Further, as compared to the untreated CLPE specimens, the PMPC-grafted CLPE specimens showed a reduction of ~84% ($p < 0.005$) in their coefficients of dynamic friction.

F7 Figure 7 shows the coefficients of dynamic friction of the untreated CLPE, PMB30-coated CLPE, PMSi90-coated CLPE, and PMPC-grafted CLPE as a function of the loads in the ball-on-plate friction test. The untreated CLPE showed the highest coefficient of dynamic friction, that is, ~0.075. This value was almost constant throughout the experiment. The coefficients of dynamic friction of the PMB30-coated

TABLE I
Surface Elemental Composition (atom %) of CLPE, MPC Polymer Coated CLPE, and PMPC Grafted CLPE ($n = 5$) AQ4

Sample	C	O	N	P	Si
CLPE (untreated)	99.8 (0.3)[a]	0.2 (0.3)	0.0 (0.0)	0.0 (0.0)	0.0 (0.0)
PMB30 coated CLPE	69.9 (1.0)	25.5 (0.6)	2.1 (0.2)	2.5 (0.3)	0.0 (0.0)
PMSi90 coated CLPE	60.5 (0.7)	30.4 (0.4)	4.1 (0.2)	4.0 (0.2)	1.0 (0.0)
PMPC grafted CLPE	58.0 (0.2)	31.5 (0.2)	5.2 (0.1)	5.3 (0.1)	0.0 (0.0)
PMPC[b]	57.9	31.6	5.3	5.3	0.0

[a] The standard deviation is in parentheses.
[b] Theoretical elemental composition of PMPC.

ID: vasanss Date: 23/4/08 Time: 21:11 Path: J:/Production/JBMM/Vol00000/080210/3B2/C2JBMM080210

J_ID: ZA1 Customer A_ID: 07-1024.R1 Cadmus Art: JBMA32092 Date: 23-APRIL-08 Stage: I Page: 6

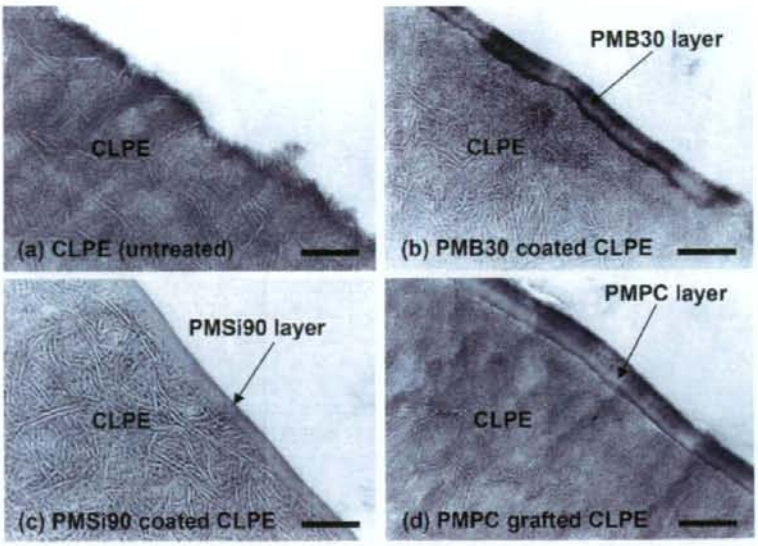

Figure 3. Cross-sectional TEM images of untreated CLPE, MPC polymer-coated CLPE, and PMPC-grafted CLPE. Bar: 200 nm.

CLPE and PMSi90-coated CLPE were smaller (~0.055) than those of the untreated CLPE at loads of up to 0.98 N; then, these coefficients increased to the level of the coefficients of the untreated CLPE at loads above 1.96 N. For both PMB30-coated CLPE and PMSi90-coated CLPE, the MPC polymer layer coating showed almost the same coefficients of dynamic friction. The PMPC-grafted CLPE showed a remarkably low friction coefficient of ~0.026 at a load of 0.49 N; this value decreased gradually and reached ~0.005 at a load of 9.80 N.

Figure 8 shows the gravimetric wear of the untreated CLPE, PMB30-coated CLPE and PMSi90-coated CLPE, and PMPC-grafted CLPE cups in the hip simulator wear test. It was observed that the wear in the PMPC-grafted CLPE cups was significantly lower than that in the untreated CLPE cups. There was no significant difference in the wear of the untreated CLPE and PMB30-coated CLPE cups. The PMSi90-coated CLPE cups showed slightly lower wear than the untreated CLPE cups; however, the weight change varied for each cup (standard F8

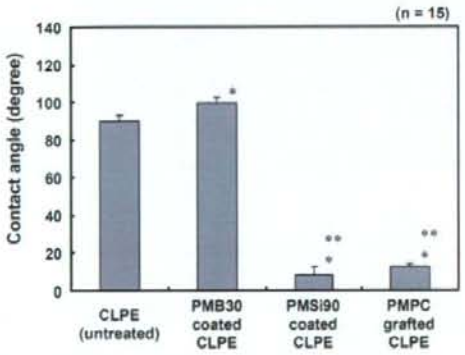

Figure 4. Static-water contact angle of untreated CLPE, MPC polymer-coated CLPE, and PMPC-grafted CLPE. Bar: Standard deviations. *: Significant difference ($p < 0.001$) as compared to the untreated CLPE, **: significant difference ($p < 0.001$) as compared to the PMB30-coated CLPE.

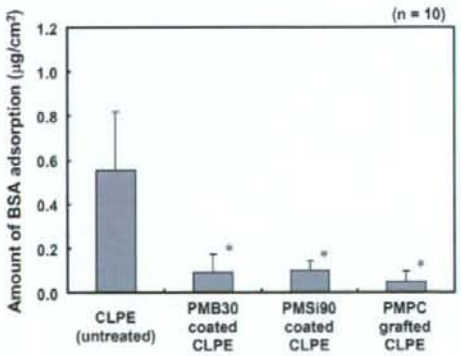

Figure 5. Amount of BSA adsorbed on the surfaces of the untreated CLPE, MPC polymer-coated CLPE, and PMPC-grafted CLPE. Bar: Standard deviations. *: Significant difference ($p < 0.001$) as compared to the untreated CLPE.

ID: vasanss Date: 23/4/08 Time: 21:11 Path: J:/Production/JBMM/Vol00000/080210/3B2/C2JBMM080210

J_ID: ZA1 Customer A_ID: 07-1024.R1 Cadmus Art: JBMA32092 Date: 23-APRIL-08 Stage: I Page: 7

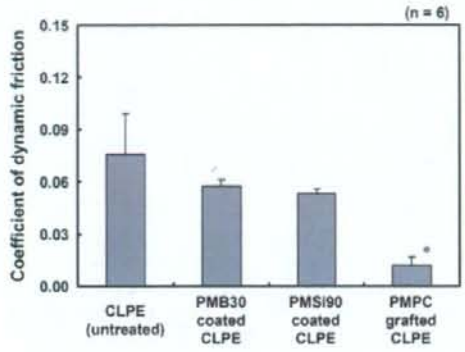

Figure 6. Coefficients of dynamic friction of untreated CLPE, MPC polymer-coated CLPE, and PMPC-grafted CLPE. Bar: Standard deviations. *: Significant difference ($p < 0.005$) as compared to the untreated CLPE.

deviation = ±9.0 mg). The PMPC-grafted CLPE cups showed a slight increase in weight. This was partially attributable to the enhanced fluid absorption in the tested cups as compared to that in the load-soak controls. While applying the gravimetric method, the weight loss in the tested cups is corrected by subtracting the weight gain in the load-soak controls; however, this correction cannot be achieved perfectly because only the tested cups are continuously subjected to motion and load. Usually, the fluid absorption in the tested cups is generally slightly higher than that in the load-soak controls. Consequently, the correction of the fluid absorption by using the load-soak data as the correction factor leads to a slight underestimation of the actual weight loss.[22,29] In this study, a steady wear rate was calculated using data from 2.0×10^6 to 3.0×10^6 cycles; in the untreated CLPE, PMB30-coated CLPE, and PMSi90-coated CLPE cups, these rates were 6.1, 5.9, and 4.5 mg/10^6 cycles, respectively. In contrast, the wear rate of the PMPC-grafted CLPE cups was markedly lower, that is, −1.5 mg/10^6 cycles.

DISCUSSION

In this study, we have investigated the surface properties of various surface modification layers formed on the CLPE surface by the physical and chemical coating of the MPC polymers or photoinduced radical grafting of MPC. Here, we discuss the durability of the CLPE whose surface is modified by the MPC polymer in terms of the characteristics of the nanometer-scale layer of the MPC polymer.

The layer, whose surface contains the physically coated PMB30, is combined with the substrate by physical adsorption.[11,12] The layer, whose surface contains the chemically coated PMSi90, is combined with the substrate by physical adsorption and/or slight Si—O—C covalent bonding ascribed to the 10% MPSi in the PMSi90 composition; a hydrolyzed silane molecule of PMSi90 has three —OH groups that react with the —OH groups of the surface oxide layer of the CLPE substrate induced by the O_2 plasma irradiation, and they form covalently siloxane bonds.[27] On the other hand, the surface modification layer obtained by PMPC grafting is combined with the substrate by strong C—C covalent bonding.[19–24]

In Figure 7, the coefficients of dynamic friction of the PMB30-coated CLPE and PMSi90-coated CLPE increased to the level of the coefficient of dynamic

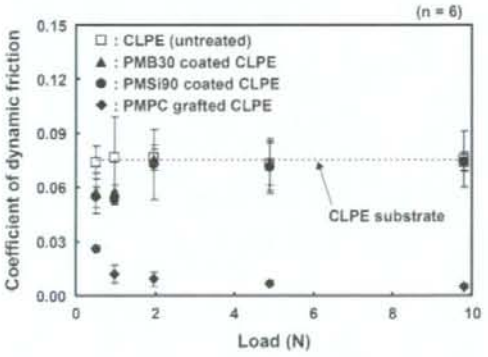

Figure 7. Coefficients of dynamic friction of the untreated CLPE, MPC polymer-coated CLPE, and PMPC-grafted CLPE as a function of loads in the ball-on-plate friction test. Bar: Standard deviations.

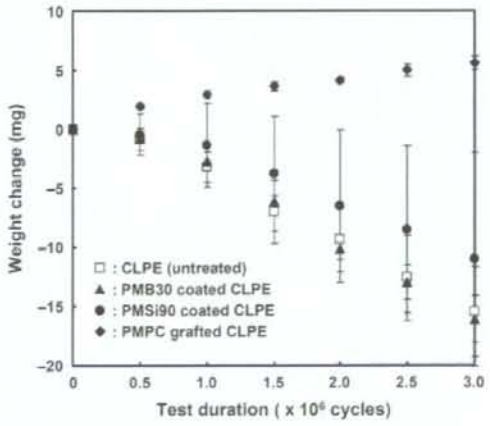

Figure 8. Weight change (volumetric wear) of the untreated CLPE, MPC polymer-coated CLPE, and PMPC-grafted CLPE in the hip joint simulator wear test. Bar: Standard deviations.

ID: vasanss Date: 23/4/08 Time: 21:11 Path: J:/Production/JBMM/Vol00000/080210/3B2/C2JBMM080210

J_ID: ZA1 Customer A_ID: 07-1024.R1 Cadmus Art: JBMA32092 Date: 23-APRIL-08 Stage: I Page: 8

friction of the untreated CLPE at loads above 1.96 N. In addition, as shown in Figure 8, there was no significant difference in the wear of the untreated CLPE and the MPC polymer coated CLPE cups in the hip joint simulator tests. In contrast, the PMPC-grafted CLPE showed an extremely low and stable coefficient of dynamic friction and volumetric wear as compared to the untreated CLPE and MPC polymer coated CLPE, as shown in Figures 7 and 8. These results indicate that the PMB30 and PMSi90 surface modification layers are removed from the CLPE surface. The surface modification layers by the PMB30 and PMSi90 coatings are combined with the substrate by physical adsorption and chemical bonds of Si—O—C, respectively. Therefore, the physical adsorption and chemical bonds of Si—O—C are ineffective in the case of large and multidirectional loads. The chemical bonds of Si—O—C are probably insufficient, because the MPSi composition in the PMSi90 polymer is 10%. Therefore, it is thought that a sufficient number of strong bonds between the surface modification layer and the CLPE surface are essential for the long-term retention of the benefits of the MPC polymer used in artificial joints under variable and multidirectional loads.

Since MPC is a highly hydrophilic compound, the MPC polymers PMSi90 and PMPC are water-soluble. The water-wettability of the PMSi90-coated and PMPC-grafted CLPE surfaces with a high MPC unit mole fraction (90 and 100%) was considerably greater than that of the untreated CLPE surface, as shown in Figure 4. Kobayashi et al. reported that the water molecules adsorbed on the surface of the highly hydrophilic PMPC act as lubricants and reduce the interaction between the PMPC and the counter-bearing face.[31] Therefore, it is thought that the artificial hip joint bearing with the PMSi90-coated and PMPC-grafted surfaces exhibited considerably higher lubricity than that with the untreated CLPE. The amount of water molecules absorbed on the surface of the CLPE (water thin-film) is expected to play an important role with regard to the property of low friction.

However, in reality fact as shown in Figure 6, the PMSi90-coated CLPE specimens exhibited a maximum reduction of ~30% in their coefficients of dynamic friction as compared to the untreated CLPE specimens. In contrast, the PMPC-grafted CLPE specimens exhibited a reduction of ~84%. It was previously reported that the polymer concentration (i.e., viscosity) increased with the friction coefficient in the mixed lubrication regime.[32] Therefore, It is assumed that an ultra-low friction of PMPC-grafted CLPE that occurs during sliding is related to the effective viscosity of the PMPC in the mixed lubrication of the intermediate hydrated layer. The high-density PMPC graft chains in the PMPC-grafted CLPE are assumed to exhibit a brush-like structure.[25,33] The viscosity of the PMPC layer reflects the mobility of the free end groups of the MPC polymer or MPC polymer chains themselves.[34,35] In contrast, the mobility of PMSi 90 is limited by the cross-linking and network entanglement of the gel structure of PMSi90. Hence, we think that the polymer brush-like structure of the PMPC-grafted CLPE with high mobility of polymer chains can function as a considerably better surface hydration lubrication system of artificial joints than the gel structure of the PMSi90-coated CLPE. These considerations are based on the previous studies on charged polymers (polyelectrolytes) by Klein and coworkers.[34,35]

The significant reduction in the coefficient of friction of the grafted PMPC resulted in a substantial improvement in wear resistance. A previous study reported that the hydrogel cartilage surface was assumed to have a brush-like structure: a part of the proteoglycan aggregate brush bonds with the collagen network in the cartilage surface.[36] It is thought that the bearing surface with high-density PMPC in artificial hip joints has a brush-like structure similar to an articular cartilage. We assume that the bearing surface of the artificial hip joint combined with a 100-nm thick MPC polymer layer results in a fluid film lubrication (or mixed lubrication) of the intermediate hydrated layer; which suggests that this novel artificial hip joint mimics the natural joint cartilage.

As shown in Figure 7, the coefficients of dynamic friction of the untreated CLPE surface were constant for all load values. In contrast, those of the PMPC-grafted CLPE surface decreased with increasing load. These results show that the PMPC-grafted layer does not follow Amonton's law of $F = \mu N$. The maximum contact stress of ~62 MPa at a load of 9.8 N is higher than the yield tensile strength of the CLPE (~23 MPa). The maximum contact stress is roughly calculated by the Hertzian theory. The elastic CLPE substrate is deformed slightly by the loads, the low friction coefficient may have been shown in order to get much more amount of water thin-film with the larger contact area of concave surface. We also think that these results imply that the lubrication of the PMPC-grafted CLPE is dominated by the hydrodynamic lubrication mechanism.

As shown in Figure 4, the static water-contact angle of the PMB30-coated CLPE was ~100°. Sibarani et al. reported that the PMB30-coated polymer surfaces showed high advancing (~100°) and low receding (~20°) contact angles.[5] Moreover, Yamasaki et al. reported that the PMB30-coated polymer surfaces required more than 30–300 min to achieve complete equilibrium.[37] This indicates that the PMB30 cannot be hydrated easily, due to the low MPC unit composition of the copolymer and low mobility of

ID: vasanss Date: 23/4/08 Time: 21:11 Path: J:/Production/JBMM/Vol00000/080210/3B2/C2JBMM080210

J_ID: ZA1 Customer A_ID: 07-1024.R1 Cadmus Art: JBMA32092 Date: 23-APRIL-08 Stage: I Page: 9

the polymer chain. However, as shown in Figure 5, the PMB30-coated CLPE surface, which could form a phosphorylcholine-enriched surface after equilibrating for 1 h, showed excellent biocompatibility as an antiadsorption surface for BSA.

The adsorption of the representative plasma protein, BSA, on the CLPE surface decreased to 9–18% due to the surface modification by the MPC polymer, as shown in Figure 5. It is hypothesized that the mechanism of protein adsorption resistivity on the surface modified by the MPC polymer is based on the water structure resulting from the interactions between water molecules and phosphorylcholine groups.[26,37,38] The large amount of free water around the phosphorylcholine group is considered to detach proteins easily and even prevent conformational changes in the adsorbed proteins.[26,38] Hence, we expect that the protein adsorption will decrease with increasing MPC unit composition in the MPC copolymer. However, in this study, there was no significant difference in the protein adsorption of the CLPE, whose surfaces was modified by the MPC polymer (the MPC unit compositions were 30, 90, and 100%). The reduction in protein adsorption is also considered to be caused by the presence of a hydrated layer around the phosphorylcholine group.[26,39] The latter consideration is consistent with the results of the water contact angle measurement, friction test, and cross-sectional TEM observations of the CLPE, whose surface is modified CLPE by the MPC polymer (Figs. 3, 4, and 6). The previous studies reported that the protein concentration of lubricants such as bovine serum considerably affected the wear rate of the UHMWPE cups in the joint simulator test: the protein concentrations in the synovial fluids of both normal and diseased joints (~20–40 mg/mL), including joints after total arthroplasty, were associated with the highest wear rates.[40,41] We think that the antiprotein adsorption surface on the CLPE prepared by the MPC polymer will prevent the highest adhesive wear rates *in vivo* caused by the protein adsorption. Moreover, the CLPE whose surface is modified by the MPC polymer is expected to exhibit tissue and blood compatibility as biocompatibility, because previous studies have reported that the MPC polymer modified surfaces exhibit *in vivo* biocompatibility.[3–11]

CONCLUSION

In this study, we systematically investigated the surface properties of the various surface modification layers formed on the CLPE surface by the MPC polymer by dip coating or photoinduced radical grafting. It is concluded that several important issues are involved in the long-term retention of the benefits of the MPC polymer used in artificial joints under variable and multidirectional loads, for example, strong bonding between the MPC polymer and the CLPE surface and high mobility of the free end groups of the MPC polymer. We should employ the photoinduced radical graft polymerization to create strong covalent bonding between the CLPE substrate and the surface modification layer, and also to retain the high mobility of polymer chains of that layer.

The authors express special thanks to Dr. Masaru Ueno (Japan Medical Materials Corp.), and Dr. Kikuko Fukumoto, Ms. Emi Tabata, and Ms. Satomi Shinbashi (The University of Tokyo) for their excellent technical assistance.

References

1. Iwasaki Y, Ishihara K. Phosphorylcholine-containing polymers for biomedical applications. Anal Bioanal Chem 2005; 381:534–546.
2. Binyamin G, Shafi BM, Mery CM. Biomaterials: A primer for surgeons. Semin Pediatr Surg 2006;15:276–283.
3. Ishihara K, Iwasaki Y, Ebihara S, Shindo Y, Nakabayashi N. Photoinduced graft polymerization of 2-methacryloyloxyethyl phosphorylcholine on polyethylene membrane surface for obtaining blood cell adhesion resistance. Colloids Surf B Biointerfaces 2000;18:325–335.
4. Kyomoto M, Iwasaki Y, Moro T, Konno T, Miyaji F, Kawaguchi H, Takatori Y, Nakamura K, Ishihara K. High lubricious surface of cobalt-chromium-molybdenum alloy prepared by grafting poly(2-methacryloyloxyethyl phosphorylcholine). Biomaterials 2007;28:3121–3130.
5. Sibarani J, Takai M, Ishihara K. Surface modification on microfluidic devices with 2-methacryloyloxyethyl phosphorylcholine polymers for reducing unfavorable protein adsorption. Colloids Surf B Biointerfaces 2007;54:88–93.
6. Ueda T, Oshida H, Kurita K, Ishihara K, Nakabayashi N. Preparation of 2-methacryloyloxyethyl phosphorylcholine copolymers with alkyl methacrylates and their blood compatibility. Polym J 1992;24:1259–1269.
7. Konno T, Ishihara K. Temporal and spatially controllable cell encapsulation using a water-soluble phospholipid polymer with phenylboronic acid moiety. Biomaterials 2007;28:1770–1777.
8. Xu Y, Takai M, Konno T, Ishihara K. Microfluidic flow control on charged phospholipid polymer interface. Lab Chip 2007;7:199–206.
9. Snyder TA, Tsukui H, Kihara S, Akimoto T, Litwak KN, Kameneva MV, Yamazaki K, Wagner WR. Preclinical biocompatibility assessment of the EVAHEART ventricular assist device: Coating comparison and platelet activation. J Biomed Mater Res A 2007;81:85–92.
10. Ueda H, Watanabe J, Konno T, Takai M, Saito A, Ishihara K. Asymmetrically functional surface properties on biocompatible phospholipid polymer membrane for bioartificial kidney. J Biomed Mater Res A 2006;77:19–27.
11. Kuiper KK, Nordrehaug JE. Early mobilization after protamine reversal of heparin following implantation of phosphorylcholine-coated stents in totally occluded coronary arteries. Am J Cardiol 2000;85:698–702.
12. Ishihara K, Ueda T, Nakabayashi N. Preparation of phospholipid polymers and their properties as polymer hydrogel membranes. Polym J 1990;22:355–360.

ID: vasanss Date: 23/4/08 Time: 21:11 Path: J:/Production/JBMM/Vol00000/080210/3B2/C2JBMM080210

13. Kurtz S, Mowat F, Ong K, Chan N, Lau E, Halpern M. Prevalence of primary and revision total hip and knee arthroplasty in the United States from 1990 through 2002. J Bone Joint Surg Am 2005;87:1487–1497.
14. Harris WH. The problem is osteolysis. Clin Orthop Relat Res 1995;311:46–53.
15. Sochart DH. Relationship of acetabular wear to osteolysis and loosening in total hip arthroplasty. Clin Orthop Relat Res 1999;363:135–150.
16. Oonishi H, Clarke IC, Good V, Amino H, Ueno M. Alumina hip joints characterized by run-in wear and steady-state wear to 14 million cycles in hip-simulator model. J Biomed Mater Res A 2004;70:523–532.
17. McMinn DJ, Daniel J, Pynsent PB, Pradhan C. Mini-incision resurfacing arthroplasty of hip through the posterior approach. Clin Orthop Relat Res 2005;441:91–98.
18. Muratoglu OK, Bragdon CR, O'Connor DO, Jasty M, Harris WH. A novel method of cross-linking ultra-high-molecular-weight polyethylene to improve wear, reduce oxidation, and retain mechanical properties. Recipient of the 1999 HAP Paul Award. J Arthroplasty 2001;16:149–160.
19. Moro T, Takatori Y, Ishihara K, Konno T, Takigawa Y, Matsushita T, Chung UI, Nakamura K, Kawaguchi H. Surface grafting of artificial joints with a biocompatible polymer for preventing periprosthetic osteolysis. Nat Mater 2004;3:829–837.
20. Moro T, Takatori Y, Ishihara K, Nakamura K, Kawaguchi H. 2006 Frank Stinchfield Award: Grafting of biocompatible polymer for longevity of artificial hip joints. Clin Orthop Relat Res 2006;453:58–63.
21. Kyomoto M, Moro T, Konno T, Takadama H, Yamawaki N, Kawaguchi H, Takatori Y, Nakamura K, Ishihara K. Enhanced wear resistance of modified cross-linked polyethylene by grafting with poly(2-methacryloyloxyethyl phosphorylcholine). J Biomed Mater Res A 2007;82:10–17.
22. Kyomoto M, Moro T, Konno T, Takadama H, Kawaguchi H, Takatori Y, Nakamura K, Yamawaki N, Ishihara K. Effects of photo-induced graft polymerization of 2-methacryloyloxyethyl phosphorylcholine on physical properties of cross-linked polyethylene in artificial hip joints. J Mater Sci Mater Med 2007;18:1809–1815.
23. Kyomoto M, Moro T, Miyaji F, Konno T, Hashimoto M, Kawaguchi H, Takatori Y, Nakamura K, Ishihara K. Enhanced wear resistance of orthopaedic bearing due to the cross-linking of poly(MPC) graft chains induced by γ-ray irradiation. J Biomed Mater Res B Appl Biomater. Forthcoming.
24. Kyomoto M, Moro T, Miyaji F, Hashimoto M, Kawaguchi H, Takatori Y, Nakamura K, Ishihara K. Effect of 2-methacryloyloxyethyl phosphorylcholine concentration on photo-induced graft polymerization of polyethylene in reducing the wear of orthopaedic bearing surface. J Biomed Mater Res A. Forthcoming.
25. Goda T, Konno T, Takai M, Moro T, Ishihara K. Biomimetic phosphorylcholine polymer grafting from polydimethylsiloxane surface using photo-induced polymerization. Biomaterials 2006;27:5151–5160.
26. Goda T, Konno T, Takai M, Ishihara K. Photoinduced phospholipid polymer grafting on Parylene film: Advanced lubrication and antibiofouling properties. Colloids Surf B Biointerfaces 2007;54:67–73.
27. ISO. Plastics-Film and sheeting-Measurement of water-contact angle of corona-treated films. International Organization for Standardization 15989, 2004.
28. ASTM F732-00: Standard test method for wear testing of polymeric materials used in total joint prostheses. In: Annual Book of ASTM Standards 13, 2004.
29. ISO. Implants for surgery: Wear of total hip-joint prostheses, Part 1: Loading and displacement parameters for wear-testing machines and corresponding environmental conditions for test. International Organization for Standardization 14242-1, 2002.
30. ISO. Implants for surgery: Wear of total hip-joint prostheses, Part 2: Methods of measurement. International Organization for Standardization 14242-2, 2000.
31. Kobayashi M, Terayama Y, Hosaka N, Kaido M, Suzuki A, Yamada N, Torikai N, Ishihara K, Takahara A. Friction behavior of high-density poly(2-methacryloyloxyethyl phosphorylcholine) brush in aqueous media. Soft Matter 2007;2:740–746.
32. de Vicente J, Stokes JR, Spikes HA. Soft lubrication of model hydrocolloids. Food Hydrocolloids 2006;20:483–491.
33. Matsuda T, Kaneko M, Ge S. Quasi-living surface graft polymerization with phosphorylcholine group(s) at the terminal end. Biomaterials 2003;24:4507–4515.
34. Raviv U, Frey J, Sak R, Laurat P, Tadmor R, Klein J. Properties and interactions of physigrafted end-functionalized poly (ethylene glycol) layers. Langmuir 2002;18:7482–7495.
35. Raviv U, Glasson S, Kampf N, Gohy JF, Jérôme R, Klein J. Lubrication by charged polymers. Nature 2003;425:163–165.
36. Ishikawa Y, Hiratsuka K, Sasada T. Role of water in the lubrication of hydrogel. Wear 2006;261:500–504.
37. Yamasaki A, Imamura Y, Kurita K, Iwasaki Y, Nakabayashi N, Ishihara K. Surface mobility of polymers having phosphorylcholine groups connected with various bridging units and their protein adsorption-resistance properties. Colloids Surf B Biointerfaces 2003;28:53–62.
38. Ishihara K, Nomura H, Mihara T, Kurita K, Iwasaki Y, Nakabayashi N. Why do phospholipid polymers reduce protein adsorption? J Biomed Mater Res 1998;39:323–330.
39. Hoshi T, Sawaguchi T, Konno T, Takai M, Ishihara K. Preparation of molecular dispersed polymer blend composed of polyethylene and poly(vinyl acetate) by in situ polymerization of vinyl acetate using supercritical carbon dioxide. Polymer 2007;48:1573–1580.
40. Wang A, Essner A, Polineni VK, Stark C, Dumbleton JH. Lubrication and wear of ultra-high molecular weight polyethylene in total joint replacements. Tribol Int 1998;31:17–33.
41. Tateiwa T, Clarke IC, Shirasu H, Masaoka T, Shishido T, Yamamoto K. Effect of low protein concentration lubricants in hip simulators. J Orthop Sci 2006;11:204–211.

AQ2

Journal of Biomedical
Materials Research
Part A

Selection of highly osteogenic and chondrogenic cells from bone marrow stromal cells in biocompatible polymer-coated plates

Journal:	*Journal of Biomedical Materials Research: Part A*
Manuscript ID:	JBMR-A-07-0733.R1
Wiley - Manuscript type:	Original Article
Date Submitted by the Author:	n/a
Complete List of Authors:	Liu, Guangyao; The University of Tokyo, Sensory & Motor System Medicine Iwata, Kumiko; The University of Tokyo, Sensory & Motor System Medicine Ogasawara, Toru; The University of Tokyo, Sensory & Motor System Medicine Watanabe, Junji; The University of Tokyo, Materials Engineering Fukazawa, Kyoko; The University of Tokyo, Department of Materials Engineering, School of Engineering, Ishihara, Kazuhiko; The University of Tokyo, Materials Engineering Asawa, Yukiyo; The University of Tokyo, Cartilage & Bone Regeneration (Fujisoft) Fujihara, Yuko; The University of Tokyo, Cartilage & Bone Regeneration (Fujisoft) Chung, Ung-il; The Univerisity of Tokyo, Bioengineering Moro, Toru; The University of Tokyo, Orthopaedic Surgery, School of Medicine Takatori, Yoshio; The University of Tokyo, Orthopaedic Surgery, School of Medicine Takato, Tsuyoshi; The University of Tokyo, Sensory & Motor System Medicine Nakamura, Kozo; Graduate School of Medicine, The University of Tokyo, Department of Sensory & Motor System Medicine Kawaguchi, Hiroshi; The University of Tokyo, Sensory & Motor System Medicine Hoshi, Kazuto; The Univeristy of Tokyo, Cartilage & Bone Regeneration (Fujisoft)
Keywords:	bone marrow stromal cell (MSC), 2-methacryloyloxyethyl phosphorylcholine (MPC) polymer , osteogenesis, chondrogenesis, cell adhesion

Selection of highly osteogenic and chondrogenic cells from bone marrow stromal cells in biocompatible polymer-coated plates

G. Liu,[1,2] K. Iwata,[1,2], T. Ogasawara,[1,2] J. Watanabe,[3] K. Fukazawa,[3] K. Ishihara,[3,4] Y. Asawa,[1] Y. Fujihara,[1] Ul. Chung,[4] T. Moro,[5] Y. Takatori,[2] T. Takato,[2] K. Nakamura,[2] H. Kawaguchi,[2] K. Hoshi[1]

[1]Department of Cartilage & Bone Regeneration (Fujisoft), Graduate School of Medicine, The University of Tokyo, Tokyo, Japan

[2]Department of Sensory & Motor System Medicine, Graduate School of Medicine, The University of Tokyo, Tokyo, Japan

[3]Department of Materials Engineering, School of Engineering, The University of Tokyo, Tokyo, Japan

[4]Deparment of Bioengineering , School of Engineering, The University of Tokyo, Tokyo, Japan

[5]Center of Disease Biology and Integrative Medicine, Graduate School of Medicine, The University of Tokyo, Tokyo, Japan

Correspondence to: K. Hoshi; e-mail: pochi-tky@umin.net

Contract grant sponcer: Grants-in-Aid for Scientific Research from the Japanese Ministry of Education, Culture, Sports, Science and Technology, Japan; contract grant numbers 18659593, 18592166.

Abstract

To enrich the subpopulation that preserves self-renewal and multipotentiality from conventionally-prepared bone marrow stromal cells (MSCs), we attempted to use 2-methacryloyloxyethyl phosphorylcholine (MPC) polymer-coated plates that selected the MSCs with strong adhesion ability and evaluated the proliferation ability or osteogenic/ chondrogenic potential of the MPC polymer-selected MSCs. The number of MSCs that were attached to the MPC polymer-coated plates decreased with an increase in the density of MPC unit (0-10%), while no significant difference in the proliferation ability was seen among these cells. The surface epitopes of CD29, CD44, CD105 and CD166, and not CD34 or CD45, were detectable in the cells of all MPC polymer-coated plates, implying that they belong to the MSC category. In the osteogenic and chondrogenic induction, the MSCs selected by the 2-5% MPC unit composition showed higher expression levels of osteoblastic and chondrocytic markers (COL1A1/ALP, or COL2A1/COL10A1/Sox9) at passage 2, compared with those of 0-1% or even 10% MPC unit composition, while the enhanced effects continued by passage 5. The selection based on the adequate cell adhesiveness by the MPC polymer-coated plates could improve the osteogenic and chondrogenic potential of MSCs, which would provide cell sources that can be used to treat the more severe and various bone/cartilage diseases.

Key words: bone marrow stromal cell (MSC), 2-methacryloyloxyethyl phosphorylcholine (MPC) polymer, osteogenesis, chondrogenesis, cell adhesion

INTRODUCTION

Bone marrow mesenchymal stem cells or stromal cells (MSCs) retain the potential to differentiate into multiple cell lineages that include osteoblasts, chondrocytes, adipocytes, myoblasts and early progenitors of neural cells.[1-3] Because MSCs can be easily obtained from a small aspirate of bone marrow and they rapidly proliferate during the early passages of the expansion culture, human MSCs are regarded as one of the attractive cell sources for regenerative medicine in bone, cartilage, heart, nerve and other tissues. However, MSCs are principally collected from bone marrow aspirates only through their selection by adhesiveness onto the plastic culture dishes,[4] and therefore, they include various subpopulations of cells which possess different proliferation rates or differentiation potentials. During the long-term culture with repeated passages, the balance among the subpopulations in the MSCs changes as a result of the difference in the proliferation rates, which may cause a deterioration of the self-renewal property or multipotentiality after repeated passages.[5]

In order to isolate or enrich the subpopulation that preserves the self-renewal and the multipotentiality from the conventionally-prepared MSCs, various kinds of efforts have been made in the past decade. It was reported that the sizes and structures of the cells could distinguish the cells possessing a great potential for multilineage differentiation, termed rapid self-renewal (RS) cells, from the heterogeneity of the MSCs.[6] The RS cells had a shaped round shape with approximately a 7 μm diameter, and could be purified by using a 10 μm filter.[6] However, some limitations had been pointed out in the paper that the filtration process could only provide a low yield of purified RS cells because the other-sized cells rapidly obstructed the filter pores. The RS cells were also characterized by the low forward scatter and low side scatter of light during a flow cytometric analysis.[7] During cell sorting with the criteria of a low forward scatter and low side scatter, the subpopulation was successfully enriched for the RS cells, which increased the differentiation potential for osteoblasts and adipocytes. Although the cell sorting technologies of flow cytometry have been highly anticipated for the

effective isolation of a specific subpopulation, some issues including the acquisition rates of target cells, the prevention of pathogen contamination, or the mechanical and thermodynamic damage to cells by the cell sorter should be cautiously evaluated before clinical use.

The MSC isolation was also attempted, using some surface epitopes, including CD13, CD29 (integrin β1), CD44 (hyaluronan receptor), CD73(SH3), CD90 (Thy-1), CD105 (Endoglin), CD166 (activated leukocyte cell adhesion molecule/ALCAM), PDGF receptor or Stro-1, all of which are highly expressed in the MSCs.[6,8] The combination with CD34 and CD45 (leukocyte common antigen/LCA), either of which is a marker of hematopoietic stem cells could exclude the hematopoietic lineage from the MSCs. However, as the expression level of the markers in the MSCs was quite similar to those of fibroblastic cells that are also contained in bone marrow aspirates and that decrease the multipotency and self-renewal,[8] specific selection of the MSCs from such heterogenetic cell populations could not be sufficiently obtained even by flow cytometry or a magnetic cell sorting system.

Serum deprivation is one of the possible methods to concentrate the subpopulation possessing a high proliferation and differentiation potential from the heterogeneity of the MSCs.[9] When early-passage human MSCs were cultured in serum-free medium without cytokines or other supplements, a subpopulation of the cells was attached to the plates and survived for 2 to 4 weeks. Afterward, such cells began to proliferate in serum-containing medium, and prominently showed stem cell properties including long telomeres or a high expression of the octomer-binding transcription factor 4 (OCT-4). The findings suggested that such cells that possess a strong adherent ability and survive in spite of the harsh environments may show a high quality of stem cell properties.

Based on this hypothesis, we attempted to select some subpopulations of MSCs showing a high adhesiveness on the culture plates. For selection, the cell adhesiveness was adjusted by the coating of 2-methacryloyloxyethyl phosphorylcholine (MPC) polymers. The MPC polymers are designed with inspiration from cell membrane surface and well-known biocompatible polymers that can reduce

protein adsorption or subsequent cell adhesion significantly.[10-12] Based on these fundamental biocompatibility, the MPC polymers have been used for preparing medical devices, for example, the surfaces of intravascular stents, intravascular guide wires, soft contact lenses, an artificial lung or artificial hip joint.[13-16] Some of these are already clinically available.

We examined the selectivity of MSCs using MPC polymer-coated plates and evaluated the proliferation ability or differentiation potential of the MPC polymer-selected subpopulation. Especially, we focused on the osteogenic and chondrogenic ability, because bone and cartilage tissue engineering using MSCs are highly desired for clinical applications.

MATERIALS AND METHODS

Preparation of MPC polymer-coated plates

Coating of the MPC polymer onto the polystyrene (PS) surface of the culture plates was performed by a simple dip-coating using MPC polymer solutions. The composition of MPC units was controlled by mixing poly(*n*-butyl methacrylate)(Poly(BMA)) and poly(MPC-*co*-BMA)(PMB30). These polymers were synthesized by a conventional radical polymerization. Poly(BMA) was a homopolymer of BMA without MPC unit (molecular weight = 4.0×10^5), and PMB30 was a copolymer composed of 30% of MPC units and 70% of BMA units (molecular weight = 6.0×10^5). In this study, the each polymer was dissolved in a mixture of tetrahydrofran (THF) and ethanol (1:9 by volume) as solvents, and then poly(BMA) and PMB30 solutions were prepared (0.25wt%). To control the MPC unit composition in the range between 0, 1, 2, 5, and 10% of MPC unit composition, these polymer mixtures in the solution were prepared. The dip-coating was carried out in the clean bench as follows: (i) 200 μL of the solution was poured into the each culture plates (ϕ 2.2cm), (ii) the polymer solution was removed after 5 seconds, (iii) the coating was repeated and the resulting culture